Catalysis Today xxx (2015) xxx–xxx

Contents lists available at ScienceDirect

Catalysis Today

journal homepage: www.elsevier.com/locate/cattod

Ex situ catalytic upgrading of lignocellulosic biomass components over vanadium contained H-MCM-41 catalysts

Beom-Sik Kim[a,1], Chang Seok Jeong[a,1], Ji Man Kim[b], Su Bin Park[b], Sung Hoon Park[c], Jong-Ki Jeon[d], Sang-Chul Jung[c], Sang Chai Kim[e], Young-Kwon Park[a,*]

[a] *School of Environmental Engineering, University of Seoul, Seoul 02504, Republic of Korea*
[b] *Department of Chemistry, Sungkyunkwan University, Suwon 16419, Republic of Korea*
[c] *Department of Environmental Engineering, Sunchon National University, Suncheon 57922, Republic of Korea*
[d] *Department of Chemical Engineering, Kongju National University, Cheonan 31080, Republic of Korea*
[e] *Department of Environmental Education, Mokpo National University, Muan 58554, Republic of Korea*

ARTICLE INFO

Article history:
Received 24 June 2015
Received in revised form 8 August 2015
Accepted 10 August 2015
Available online xxx

Keywords:
Ex situ catalytic pyrolysis
Components of lignocellulosic biomass
Vanadium
H-V-MCM-41
Valuable chemicals

ABSTRACT

H-V-MCM-41 catalysts containing 5, 10, and 30 wt% of vanadium were synthesized and applied to the *ex situ* catalytic pyrolysis (CP) of three polymeric components of lignocellulosic biomass for the first time. Characterization of the catalysts was performed using N_2 adsorption–desorption, XRD, FT-IR, and NH_3-TPD. The results of XRD analysis showed that 5 wt% and 10 wt% H-V-MCM-41 catalysts maintained the mesoporous structure, whereas the mesoporous structure was destroyed in 30 wt% H-V-MCM-41 with considerable amount of small V_2O_5 crystalline outside the framework. NH_3-TPD showed that H-V-MCM-41 has mostly weak acid sites and that 10 wt% H-V-MCM-41 had the largest quantity of acid sites due to framework vanadium. In the case of CP of cellulose using Py-GC/MS, 10 wt% H-V-MCM-41 showed the highest catalytic activity for the production of valuable furanic compounds such as furfural because of the enhanced deoxygenation over the acid sites formed on framework vanadium. In the case of CP of xylan as well, 10 wt% H-V-MCM-41 led to the largest yield of mono-aromatics. The production of acetic acid was also promoted by H-V-MCM-41 catalysts. The CP of lignin over H-V-MCM-41 catalysts promoted substantially the production of important feedstock chemicals for the petrochemical industry: phenolics and mono-aromatics.

1. Introduction

Production of various biofuels, biomaterials and biochemicals from lignocellulosic biomass has recently received significant attention [1–7]. Among other processes, fast pyrolysis can produce bio-oil containing hundreds of chemicals. However, the bio-oil produced from pyrolysis has large oxygen content, is very acidic with pH of 2–3, and has low stability, e.g. viscosity increase due to reactions of the chemicals upon long storage [8–11]. Coexistence of a large number of chemicals with low fractions makes it difficult to selectively separate valuable components. Therefore, reforming of the bio-oil is required to improve the oil quality by increasing the contents of valuable components.

Catalytic pyrolysis (CP) using various catalysts is a promising way to produce bio-oil with low O_2 amount and high stability [12–15]. CP also leads to increased contents of valuable species, such as furans, mono-aromatics, and light phenolics because the reaction intermediates produced from thermal pyrolysis are converted selectively to high-value-added compounds by catalysis. CP of a variety of lignocellulosic biomass materials has been carried out using different catalysts: zeolites, mesoporous materials, and metal oxides [12–15]. In addition, CP could be classified into *in situ* CP and *ex situ* CP depending on the contact type between catalyst and biomass [14]. Biomass and catalyst were mixed together in a reactor for *in situ* CP, whereas pyrolytic vapor produced from thermal transformation in a separate pyrolyzer was allowed to contact with catalyst located on downstream of pyrolyzer for *ex situ* CP. Lignocellulosic biomass is composed mostly of three kinds of polymeric components: cellulose (30–50%), hemicellulose (15–35%), and lignin (10–20%) [16–18]. Therefore, it is needed to examine the CP of these components as well as various biomass materials to enhance our understanding on the CP behavior of lignocellulosic biomass. Thus far, however, research on the CP of these biomass components is relatively rare, whereas lots of studies have been conducted on the CP of a variety of lignocellulosic biomass materials. In addition,

* Corresponding author.
E-mail address: catalica@uos.ac.kr (Y.-K. Park).
[1] Co-first authors.

http://dx.doi.org/10.1016/j.cattod.2015.08.031
0920-5861/

most CP studies of biomass components have used microporous zeolites, e.g. HZSM-5, HY, and HBeta [17,19–24], while the application of mesoporous materials (e.g. Al-SBA-15, Al-MCM-41, etc.) [25–30], metal oxides (e.g. SiO_2, MgO, Al_2O_3, TiO_2, etc.) [31], and metal chloride ($CuCl_2$, etc.) [32], is very limited. Mesoporous catalysts containing various metal components are expected to be effective for the catalytic conversion of large molecules contained in bio-oil, calling for further research efforts in this field.

Vanadium is an effective catalyst material for various reactions including selective catalytic reduction, VOC oxidation, and oxidative dehydrogenation. Therefore, it is expected that vanadium-based catalysts have high catalytic activity for biomass pyrolysis. However, vanadium-containing catalysts have been used neither for *ex situ* CP of lignocellulosic biomass materials nor for that of biomass components.

In this study, H-V-MCM-41 catalysts were synthesized by incorporating vanadium within a representative mesoporous material MCM-41 and applied to the *ex situ* CP of biomass components, for the first time, aiming at enhancing the production of valuable chemicals.

2. Experimental

2.1. Samples

Commercial cellulose, xylan (model compound of hemicellulose), kraft lignin, and levoglucosan were purchased from Sigma–Aldrich.

2.2. Synthesis of H-V-MCM-41

Highly ordered mesoporous silica MCM-41 was synthesized by the following procedure. Cetyltrimethylammonium bromide (CTAB, 24.29 g, 99+%, ACROS) were dissolved in distilled water (280 g). Then, sodium silicate solution (100 g, 20 wt% SiO_2, Na/Si = 0.5) were added to the CTAB solution at room temperature drop by drop. The mixture was vigorously stirred for 1 h at room temperature and aged in an oven at 100 °C for 24 h. Then, the mixture was cooled down at room temperature and pH was adjusted to 10 by using 50 wt% aqueous acetic acid solution. The mixture was reheated at 100 °C for 48 h. The cooling – pH adjustment – aging process was repeated two more times. The reaction mixture was filtered, washed with distilled water, and dried at 80 °C for 24 h. Dried powder was washed with HCl (36 wt%, SAMCHUN)-dissolved ethanol solution, and dried in the 80 °C oven for 24 h. Finally, the product was calcined at 550 °C for 3 h in air. In order to introduce catalytic activities on mesoporous silica (MCM-41), vanadium was incorporated into MCM-41 with various ratios. Before adding sodium silicate solution, vanadyl sulfate hydrate, $VOSO_4{\cdot}xH_2O$ (97 wt%, Sigma–Aldrich), was added to the solution. The rest of synthetic procedure was the same. The target doping ratios of vanadium were 5, 10, and 30 wt%; therefore, corresponding added masses of $VOSO_4{\cdot}xH_2O$ were 1.8479, 3.6958, and 11.0875 g, respectively.

Ion exchanges of V-MCM-41 with different vanadium contents were carried out with aqueous solution of 2 M NH_4Cl (98.5%, SAMCHUN). Calcined mesoporous silica (3 g) was added to aqueous solution of 2 M NH_4Cl (0.5 L), and the mixture was vigorously stirred at 80 °C for 24 h. Resulting powders were filtered, washed with distilled water, and dried for 24 h in the 80 °C oven. After drying samples, they were calcined for 3 h at 500 °C. Finally obtained catalyst was named H-V-MCM-41.

2.3. Characterization of catalysts

Wide-angle X-ray diffraction (XRD) patterns and small-angle X-ray scattering (SAXS) patterns were obtained using Rigaku Ultima III (a Cu Kα X-ray at 30 kV, 40 mA) and using Rigaku D/Max-2500 (a Cu Kα X-ray at 40 kV, 300 mA), respectively. Surface area and pore size distribution were derived from the N_2 adsorption–desorption isotherms prepared by Micromeritics Tristar 3000 at −196 °C (liquid N_2), using Brunauer–Emmett–Teller (BET) model and Barrett–Joyner–Halenda (BJH) method, respectively. Scanning electron microscopy (SEM) images were obtained using JEOL JEM-7100F at an accelerating voltage of 15 kV. The acidities of the catalysts were examined using ammonia-temperature programmed desorption (NH_3-TPD) conducted from room temperature to 700 °C with a rising rate of 10 °C/min. First, 0.1 g of catalyst sample was heated for 30 min at 200 °C in a 40-ml/min He gas flow. The adsorption of NH_3 on the catalyst surface was then conducted by flowing 4.9 wt% NH_3/He gas for 1 h at room temperature. NH_3 desorbed during the temperature rising was detected using a thermal conductivity detector. Fourier transform infrared (FT–IR) spectroscopy was carried out through Bruker VERTEX 70 in the range of 4000–400 cm^{-1} at room temperature. FT–IR spectra are measured by KBr wafer technique.

2.4. Ex situ *CP using Py-GC/MS*

Pyrolysis experiments were performed using Py-GC/MS, which is a combination of a vertical furnace type pyrolyzer (Py-2020D, Frontier-Lab Co.) and GC (Agilent 7890A Gas Chromatography)/MS (Agilent 5975C inert Mass Spectral Detector). The biomass components and catalyst were placed in a metal sample cup to be inserted into a heated pyrolyzer. For each pyrolysis experiment, 1 mg of biomass component was placed in the cup. In the case of CP, 1 mg of catalyst was added over the biomass component sample layer, with a quartz wool layer located in-between separating the biomass and catalyst layers. In this arrangement, non-catalytic pyrolysis (non-CP) and reforming occur sequentially; the vapor product produced from non-CP is reformed when it passes through the catalyst layer. Helium gas with a split ratio of 50:1 was used as the carrier gas flowing through the reactor.

Each pyrolysis experiment was conducted for 3 min at 500 °C. The pyrolysis product was analyzed by the GC/MS equipped with an ultra alloy-5 column (30 m × 0.25 mm × 0.5 mm). MicroJet cryotrap was used to analyze volatile components with high resolution. The pyrolysis product gas was condensed using liquid nitrogen for 3 min and introduced into the column by thermal desorption. The GC/MS interface temperature was set at 300 °C and the GC oven temperature was programmed to increase from 40 °C to 320 °C with a rate of 5 °C/min. Including the constant-temperature periods of 4 min and 10 min, respectively, before and after the temperature rising, the total analysis time was 70 min. The mass spectra picks were interpreted using the NIST05 library.

In order to examine the effects of catalyst dose, additional experiments were carried out changing the quantity of catalyst used for each experiment, with the other conditions remaining unchanged.

3. Results and discussion

3.1. Characterization of catalysts

Fig. 1 shows low angle and high angle XRD patterns of synthesized H-V-MCM-41 catalysts. 5 and 10 wt% H-V-MCM-41 have 2-D hexagonal pore structure diffraction patterns (2θ = 0.4–10°) and diffraction line of amorphous silica. The XRD pattern of 30 wt% H-V-MCM-41 indicates that 2-D hexagonal pore structure was almost collapsed due to crystallization of V_2O_5 leaving a disordered pore structure (inferred from N_2 adsorption–desorption isotherm of 30 wt% H-V-MCM-41 in Fig. 2). Also, V_2O_5 nanoparticles were detached from silica frameworks during heat treatment. Therefore,

Please cite this article in press as: B.-S. Kim, et al., *Ex situ* catalytic upgrading of lignocellulosic biomass components over vanadium contained H-MCM-41 catalysts, Catal. Today (2015), http://dx.doi.org/10.1016/j.cattod.2015.08.031

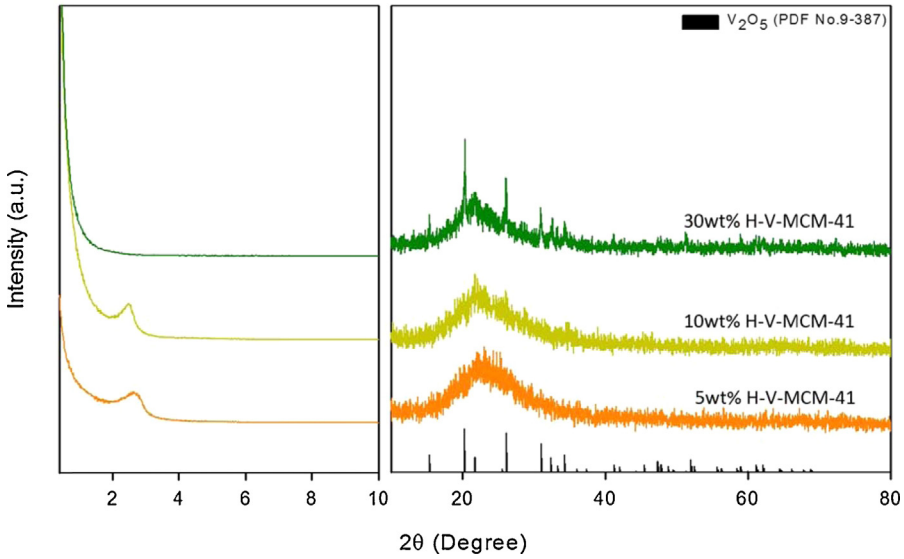

Fig. 1. X-ray diffraction (XRD) patterns of H-V-MCM-41.

high angle diffraction pattern of 30 wt% H-V-MCM-41 showed crystallized V_2O_5 diffraction peaks while two other samples with low vanadium loadings did not. The grain size (85.4 nm) of V_2O_5 nanoparticles in 30 wt% H-V-MCM-41 was obtained from Scherrer equation through deconvolution process using PDXL2 (Software, Rigaku). The grain size of bulk V_2O_5 powder was calculated to be 206.2 nm (data not shown).

In Fig. 2, N_2 adsorption–desorption isotherms show that the H-V-MCM-41 catalysts have typical type-IV isotherms which are characteristics of mesoporous materials. BET surface area of synthesized materials decreased from 889 to 113 m^2/g, and total pore volume decreased from 0.53 to 0.27 cm^3/g (0.74 cm^3/g for 10 wt% H-V-MCM-41) with increasing doped vanadium content from 5 wt% to 30 wt%. Pore sizes increased from 1.6 nm to 2.8 nm when the quantity of doped V_2O_5 increased from 5 wt% to 30 wt%. The results of N_2 adsorption–desorption analysis were summarized in Table 1.

Table 1
Physical properties of H-V-MCM-41 catalysts.

Material	S_{BET} (m^2/g)	V_{Total} (cm^3/g)	Pore size (nm)
5 wt% H-V-MCM-41	889	0.53	1.6
10 wt% H-V-MCM-41	634	0.74	2.0
30 wt% H-V-MCM-41	113	0.27	2.8

As shown in Fig. 3, the synthesized materials had no unique morphologies such as sphere, rod, plate, etc. It must be pointed out that 30 wt% H-V-MCM-41 sample (Fig. 3A) demonstrated the different morphology from the others, which is explained by the fact that 2-D hexagonal pore structure was collapsed by V_2O_5 crystallization. The higher resolution image embedded in Fig. 3C indicates that small nanoparticles (of which diameter is around 80–90 nm) are V_2O_5 nanoparticles detached from MCM-41 silica framework. In order to calculate the mass content of V_2O_5 versus SiO_2,

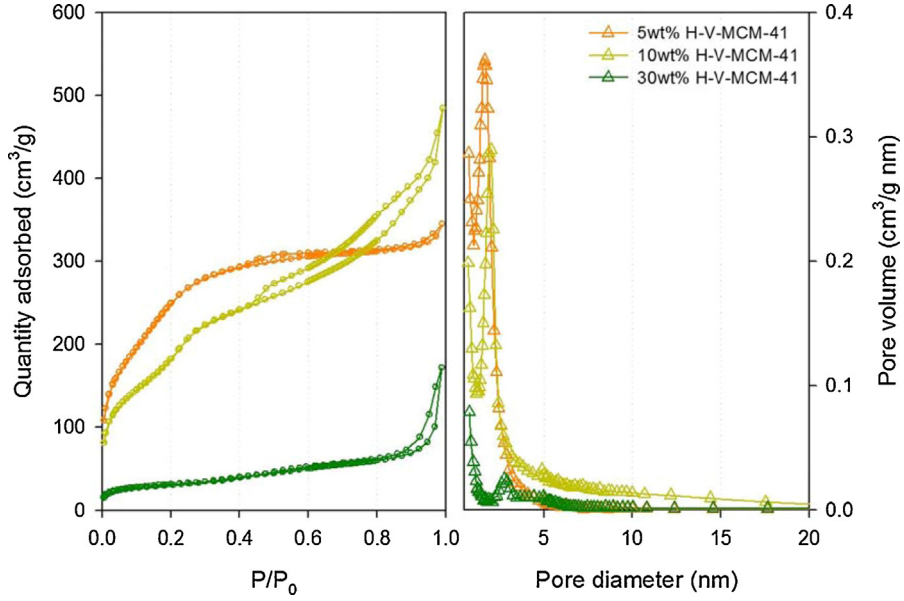

Fig. 2. N_2 adsorption–desorption isotherms and pore size distributions of H-V-MCM-41.

Please cite this article in press as: B.-S. Kim, et al., *Ex situ* catalytic upgrading of lignocellulosic biomass components over vanadium contained H-MCM-41 catalysts, Catal. Today (2015), http://dx.doi.org/10.1016/j.cattod.2015.08.031

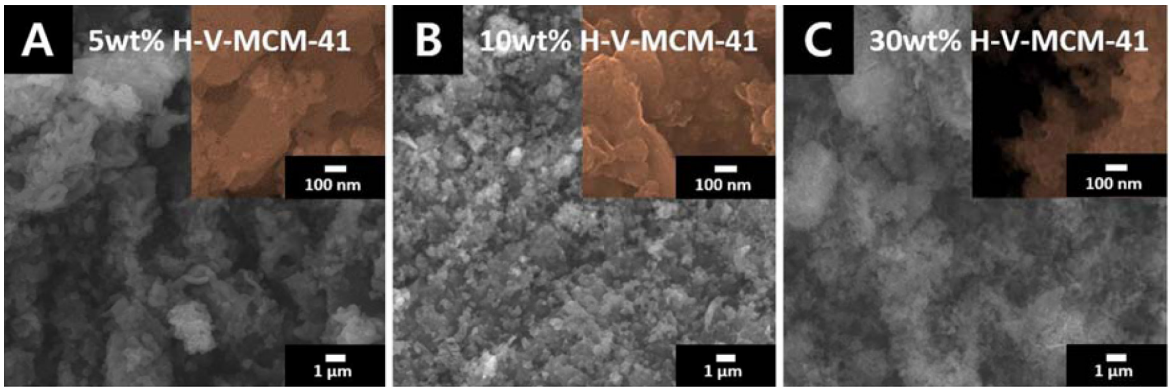

Fig. 3. SEM images of H-V-MCM-41: A. 5 wt%, B. 10 wt%, and C. 30 wt% H-V-MCM-41.

Table 2
V doping ratio calculation by SEM EDS data.

H-V-MCM-41 (wt%)	SiO_2 (g)	V_2O_5 (g)	O (atomic %)	Si (atomic %)	V (atomic %)	wt% cal.
5	1830.14	13.64	69.39	30.46	0.15	0.74
10	1394.39	47.29	76.27	23.21	0.52	3.28
30	1838.75	471.68	64.21	30.60	5.19	20.42

energy-dispersive X-ray spectroscopy (EDS) was used, and the result and calculations were summarized in Table 2. Approximately calculated doping ratios of V_2O_5 are different from the ratios of added vanadium precursors. The vanadium content in H-V-MCM-41 increased with increasing quantity of vanadium precursor added. The difference between added amount of vanadium precursor and the vanadium content in H-V-MCM-41 may stem from the washing process using HCl-ethanol solution during V-MCM-41 synthesis because vanadium precursors are very easily dissolved into acidic solutions.

In order to confirm Si—O—V bonding in H-V-MCM-41 framework, FT-IR spectroscopy was carried out, and FT-IR spectra are shown in Fig. 4. All samples have the band at 464 cm^{-1} and 796 cm^{-1} due to Si—O stretching and tetrahedron bonding. Also, they exhibit the band at 1090 cm^{-1} and 1230 cm^{-1} of Si—O—Si vibrations. 5 and 10 wt% H-V-MCM-41 have two absorption bands near 3400 cm^{-1} and 1635 cm^{-1} originating from —OH groups of silanol and water molecules, respectively [33]. A band at 960 cm^{-1} is assigned to the Si—O stretching vibration due to Si—O—R (R = H, hetero atoms such as transition metals, etc.) [34,35]. Therefore, the band at 956 cm^{-1} means that Si—O—V stretching vibrations exist in H-V-MCM-41 framework in Fig. 4. In FT-IR spectrum of 30 wt% H-V-MCM-41, Si—O—V stretching peak is shifted to lower wavenumber, and wavenumber of Si—O stretching peak is increased. Also, the intensity of the band at 956 cm^{-1} of 30 wt% H-V-MCM-41 was decreased. It means that there are less Si—O—V bonds in 30 wt% H-V-MCM-41 rather than in 5 and 10 wt% H-V-MCM-41. In comparison with XRD patterns in Fig. 1, V atoms are well inserted into MCM-41 framework to form Si—O—V bonding in cases of 5, 10 and 30 wt% H-V-MCM-41, but V_2O_5 nanoparticles were also generated in case of 30 wt% H-V-MCM-41.

NH_3-TPD profiles of H-V-MCM-41 are shown in Fig. 5. The amount of adsorbed NH_3 is related to the acidity of catalyst surface. Strongly bounded NH_3 are desorbed at higher temperature, which means that the catalyst has higher acidity. Also, the intensity of NH_3-TPD profile means how many NH_3 molecules were adsorbed on sites. In Fig. 5, 5 and 10 wt% H-V-MCM-41 have peaks at 120 and 124 °C. This is because NH_3 molecules were adsorbed on H^+ ion on Si—O—V frameworks of H-V-MCM-41. In case of 30 wt% H-V-MCM-41, NH_3-TPD profile shows unique and stronger peaks at 180 °C and at 222 °C, and a shoulder-like peak near 120 °C. The shoulder-like

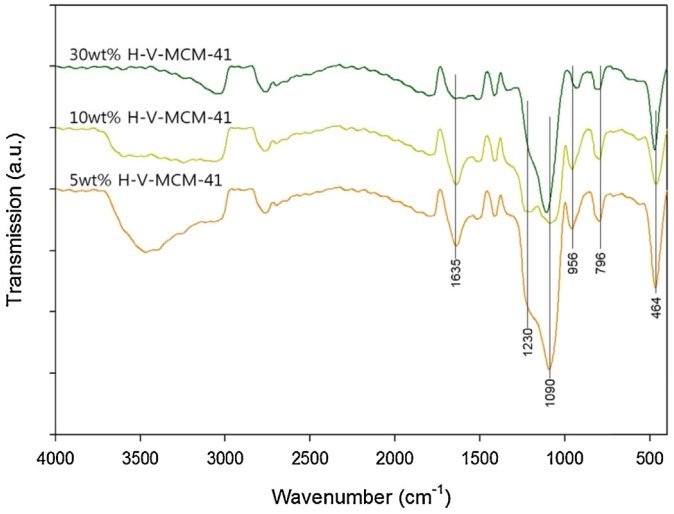

Fig. 4. FT-IR spectra of H-V-MCM-41 catalysts.

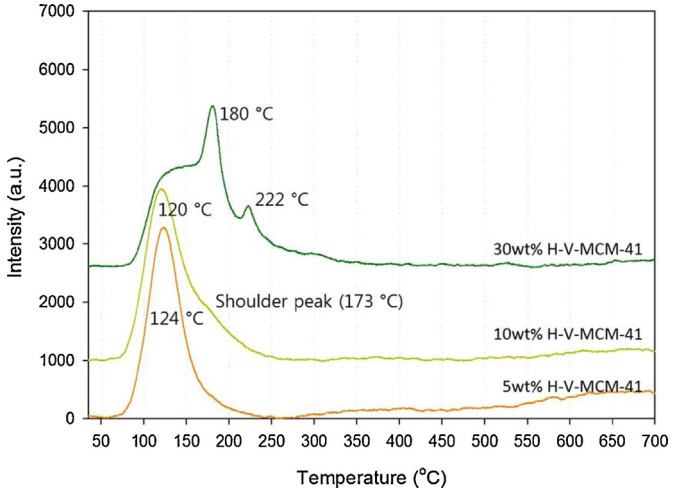

Fig. 5. NH_3-TPD profiles of H-V-MCM-41.

Please cite this article in press as: B.-S. Kim, et al., *Ex situ* catalytic upgrading of lignocellulosic biomass components over vanadium contained H-MCM-41 catalysts, Catal. Today (2015), http://dx.doi.org/10.1016/j.cattod.2015.08.031

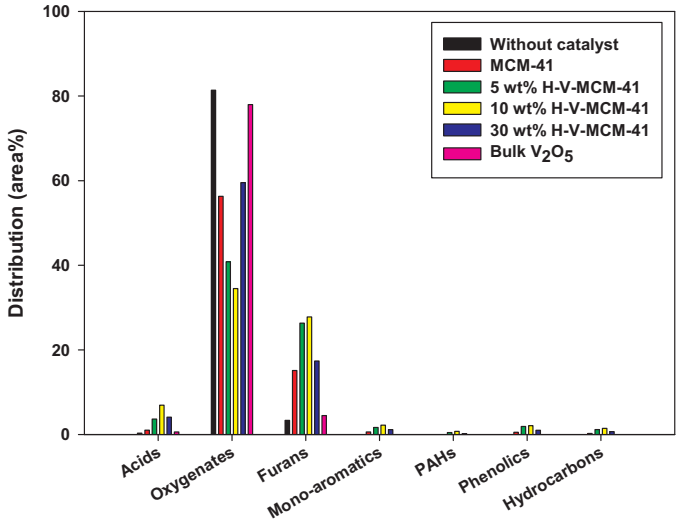

Fig. 6. Product distribution of catalytic pyrolysis of cellulose over H-V-MCM-41 catalysts.

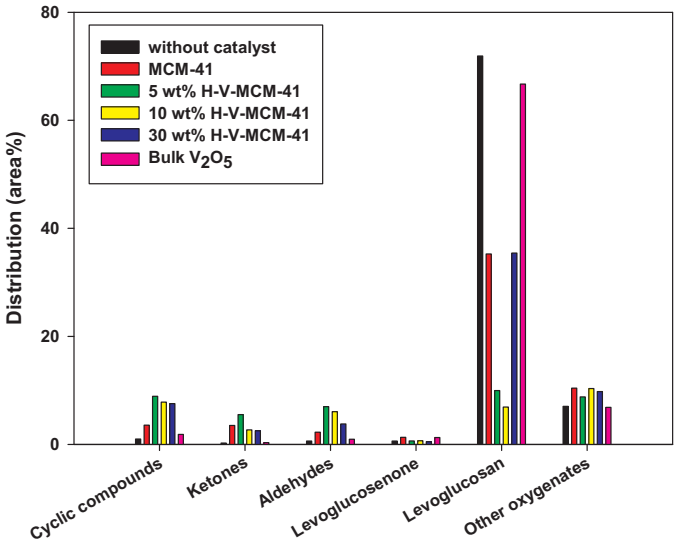

Fig. 7. Product distribution of oxygenates via catalytic pyrolysis of cellulose over H-V-MCM-41 catalysts.

peak near 120 °C would be from H^+ ion on Si—O—V frameworks of H-V-MCM-41. In contrast, the peaks at 180 °C and 222 °C imply the existence of V_2O_5 nanoparticles detached from Si—O—V frameworks. Therefore, 30 wt% H-V-MCM-41 has higher acidity than 5 and 10 wt% H-V-MCM-41 due to V_2O_5 nanoparticles.

3.2. Ex situ *CP*

3.2.1. Ex situ *CP of cellulose*

Fig. 6 shows the results of the CP of cellulose over H-V-MCM-41. All the species contained in the product bio-oil were grouped into acids (including acetic acid), oxygenates (including levoglucosan), furanic compounds (furans), mono-aromatics, polycyclic aromatic hydrocarbons (PAHs), phenolics, and hydrocarbons. The CP of cellulose over H-V-MCM-41 resulted in decreased oxygenates, compared to non-CP, while the other components increased. In particular, the content of furans in the bio-oil obtained from CP over 10 wt% H-V-MCM-41 was about 28%, which was more than 7 times larger than that from non-CP. The oxygenate conversion was high especially for 5 wt% H-V-MCM-41 and for 10 wt% H-V-MCM-41, which maintained the MCM-41 structure after the vanadium insertion. Meanwhile, 30 wt% H-V-MCM-41, in which significant destruction of MCM-41 structure was observed after the vanadium insertion, exhibited similar catalytic activity with Si-MCM-41, having no acid sites. As shown in the NH_3-TPD result (Fig. 5), 5 wt% and 10 wt% H-V-MCM-41 catalysts had less quantities of acid sites than 30 wt% H-V-MCM-41. However, most vanadium-based acid sites in 5 wt% and 10 wt% H-V-MCM-41 may be due to the framework vanadium of V-MCM-41. On the contrary, in 30 wt% H-V-MCM-41, most vanadium existed as V_2O_5 particles outside the MCM-41 framework, acting only as Lewis acid sites with weak catalytic activity. Therefore, the quantity of vanadium-based acid sites due to framework vanadium is apparently a more important parameter than the total quantity of acid sites. When bulk V_2O_5 particles were used for the CP of cellulose, the catalytic activity was even much lower than that of 30 wt% H-V-MCM-41, which was attributed to the larger particle size of V_2O_5 (206 nm) than that of vanadium incorporated into 30 wt% H-V-MCM-41 (80 nm).

Fig. 7 shows the detailed species distribution of oxygenates. The most abundant product of the non-CP of cellulose was levoglucosan, a large part of which was removed by catalytic reforming. Because levoglucosan is known to be converted to other species such as furans owing to dehydration in the presence of acid sites

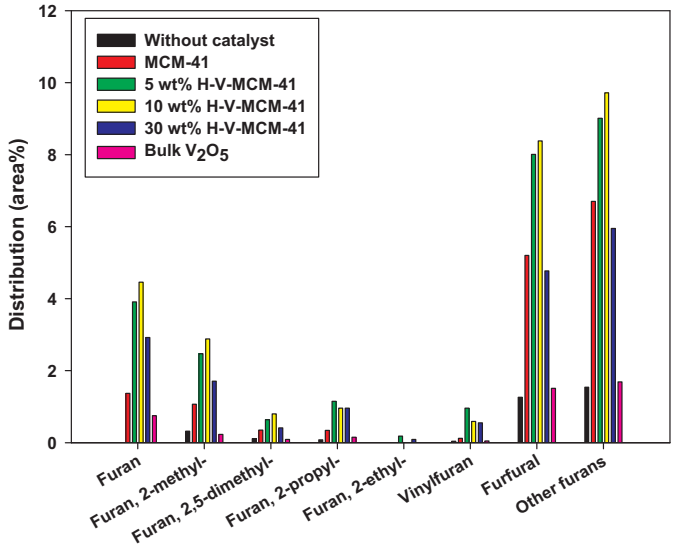

Fig. 8. Product distribution of furans via catalytic pyrolysis of cellulose over H-V-MCM-41 catalysts.

[19,26,29,30], the high conversion of levoglucosan observed in the CP over 5 wt% and 10 wt% H-V-MCM-41 was attributed to the acid sites due to framework vanadium of V-MCM-41. On the other hand, 30 wt% H-V-MCM-41 showed similar levoglucosan conversion to that of MCM-41 with no acid sites. This indicates that the extra-framework vanadium-based acid sites existing in 30 wt% H-V-MCM-41 play a nearly negligible role in the conversion of levoglucosan.

The bulk V_2O_5 particles showed virtually no catalytic activity, indicating bulk V_2O_5 is inferior to smaller V_2O_5 particle-based catalysts (e.g. 30 wt% H-V-MCM-41) in terms of the production of furans.

Fig. 8 shows the detailed species distribution of furanic compounds. The most abundant furanic compound was furfural. Catalytic reforming considerably enhanced the production of alkylated furans, such as furan, 2-methyl furan, 2-propyl furan, and 2,5-dimethyl furan, which were hardly produced from non-CP. This result was attributed to the enhanced dehydration and decarbonylation of levoglucosan occurring on the acid sites of H-V-MCM-41.

Please cite this article in press as: B.-S. Kim, et al., *Ex situ* catalytic upgrading of lignocellulosic biomass components over vanadium contained H-MCM-41 catalysts, Catal. Today (2015), http://dx.doi.org/10.1016/j.cattod.2015.08.031

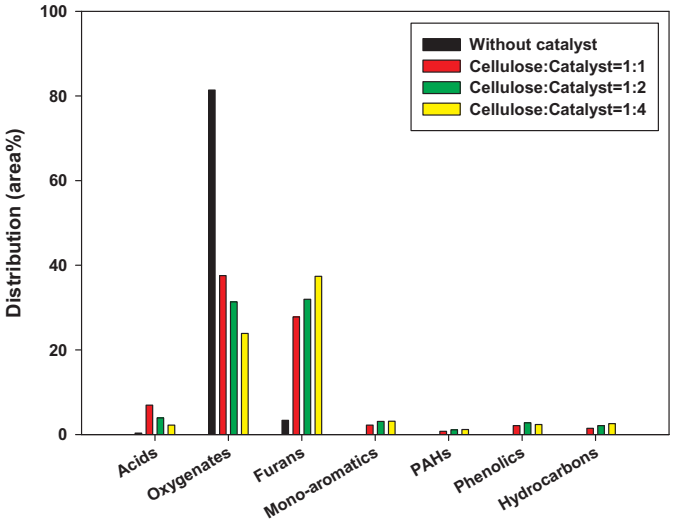

Fig. 9. Effect of catalyst amount on the product distribution of catalytic pyrolysis of cellulose over 10 wt% H-V-MCM-41.

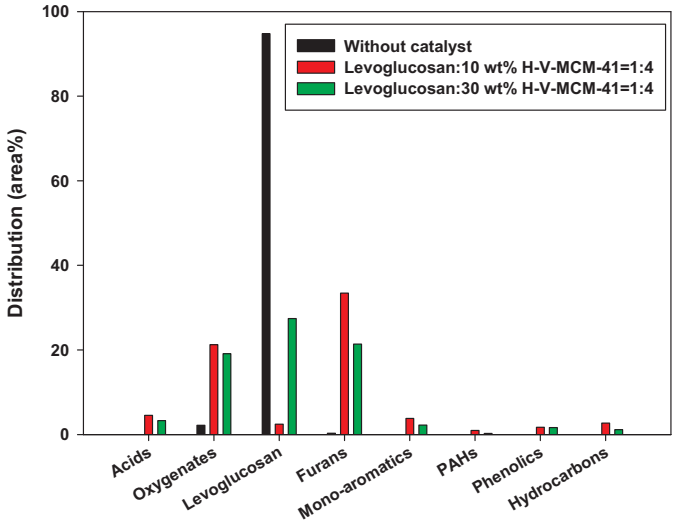

Fig. 10. Catalytic pyrolysis of levoglucosan over 10 wt% H-V-MCM-41 and 30 wt% H-V-MCM-41.

Furfural, whose global production is about 250,000 tones/year, is an important chemical used in the production of various materials, e.g. furanic resin, pesticide, solvent, and plastics [36]. Therefore, the enhanced production of furfural by catalysis is beneficial to improve the economy of the pyrolysis process. Again 5 wt% and 10 wt% H-V-MCM-41 showed much higher enhancement in the production of furans than 30 wt% H-V-MCM-41. The catalytic activity of bulk V_2O_5 particles was negligible again.

Fig. 9 compares the results obtained with different doses of 10 wt% H-V-MCM-41. With increasing catalyst dose, the fraction of oxygenates decreased, while that of furanic compounds increased. The conversion of levoglucosan increased with increasing catalyst dose. When the catalyst/biomass ratio was 4, most levoglucosan was removed. It is believed that levoglucosan was converted, via dehydration and decarbonylation, into furanic compounds and, via cracking and aromatization, into mono-aromatics and hydrocarbons. Among the furanic compounds, the fractions of furfural and alkylated furans, with high value-added, were increased considerably with increasing catalyst dose, probably due to increased acid sites.

Mono-aromatics, which were not produced from the non-CP of cellulose, was produced by catalytic reforming over H-V-MCM-41, being 2.1% when 10 wt% H-V-MCM-41 was used. When the catalyst/biomass ratio was increased to 4, the fraction of mono-aromatics increased to 3.1%. Nevertheless, this fraction of mono-aromatics was relatively low because the acidity H-V-MCM-41 was relatively weak. Furanic compounds including furfural are known to be converted to aromatics on strong acid sites [19,26,37,38]. Therefore, high fraction of furanic compounds accompanying with low fraction of aromatics obtained in this study can be attributed to weak acidity of H-V-MCM-41. In a previous study on CP of biomass over mesoporous materials, furanic compounds are dominantly produced over aromatics [29,30,39], which is in good agreement with the result of this study.

To investigate more deeply the conversion of levoglucosan, which is the most important reaction intermediate of the pyrolysis of cellulose, the conversion reaction of levoglucosan was converted over 10 wt% H-V-MCM-41 and 30 wt% H-V-MCM-41. As shown in Fig. 10, the conversion of levoglucosan was negligible without catalyst with less than 5% conversion, whereas 10 wt% H-V-MCM-41 converted most levoglucosan and 30 wt% H-V-MCM-41 converted 72.6% of levoglucosan. This result confirmed that the acid sites based on framework vanadium play an important role in the conversion of levoglucosan. As was mentioned above, levoglucosan was converted mostly into furanic compounds (furfural, alkylated furans, etc.) and partly into mono-aromatics, hydrocarbons, and acids, over H-V-MCM-41 with weak acid sites.

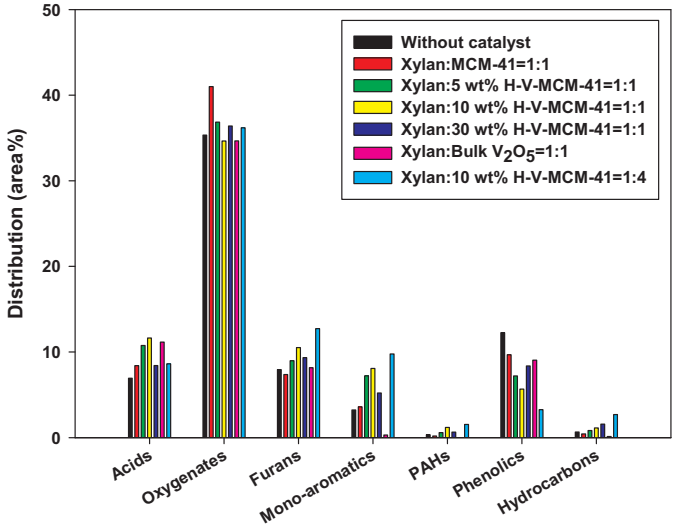

Fig. 11. Product distribution of catalytic pyrolysis of xylan over H-V-MCM-41 catalysts.

3.2.2. Ex situ *CP of xylan*

Fig. 11 shows the product species distribution obtained from the pyrolysis of xylan (hemicellulose). Compared to the pyrolysis of cellulose, in which levoglucosan was the most abundant product of non-CP, the pyrolysis of xylan produced the oxygenates as major species, followed by acids, furans, mono-aromatics, and phenolics. Because xylan is more structurally unstable than crystalline cellulose [40], its thermal decomposition takes place more easily. The fraction of acids was particularly high (6.9%), compared to the pyrolysis of cellulose (0.3%), owing to the production of acetic acid from the decomposition of O-acetal functional groups in xylan [29,30]. CP of xylan increased the fraction of acids even further through additional decomposition reactions. In particular, the fraction of acids was almost doubled (11.6%) over 10 wt% H-V-MCM-41. Acetic acid and formic acid were the two most abundant acids; the

Please cite this article in press as: B.-S. Kim, et al., *Ex situ* catalytic upgrading of lignocellulosic biomass components over vanadium contained H-MCM-41 catalysts, Catal. Today (2015), http://dx.doi.org/10.1016/j.cattod.2015.08.031

fraction of acetic acid was 68%. Because acetic acid is an important species used for the production of various chemicals, further research is needed to enhance its production.

Another important product species group of the CP of xylan is mono-aromatics. Being C6-C8 aromatics, benzene, toluene, ethylbenzene, and xylene, among other mono-aromatics, are important building compounds used in the petrochemical industry. Therefore, promoting the production of these species is one of the most important goals in the CP of biomass. Catalytic reforming over 5 wt% and 10 wt% H-V-MCM-41 catalysts increased the production of mono-aromatics from xylan by a factor of larger than two; the fraction of mono-aromatics increased from 3.2% for non-CP to 7.2% for the CP over 5 wt% H-V-MCM-41 and to 8.1% for the CP over 10 wt% H-V-MCM-41. The CP over MCM-41 having few acid sites resulted in the mono-aromatics fraction of 3.6%, which is similar to the value obtained from non-CP. Therefore, the acidity of H-V-MCM-41 appeared to be an important parameter in the conversion of xylan. Generally, various reaction intermediates produced during the pyrolysis of biomass (acids, aldehydes, anhydrosugars, etc.) undergo cracking, deoxygenation, oligomerization, and aromatization in the presence of acid sites, eventually resulting in the production of mono-aromatics. 30 wt% H-V-MCM-41, with the largest quantity of acid sites, led to lower fraction of mono-aromatics (5.2%) than 5 wt% and 10 wt% H-V-MCM-41 catalysts although it was higher than that obtained from non-CP or the CP over MCM-41, confirming again the important role of the acid sites based on framework vanadium (V—O—Si).

Hemicellulose is also known to be converted to furanic compounds via dehydration over acidic catalysts [37]. Current study also showed that the CP of xylan increased the production of furanic compounds compared to non-CP. The margin of increase, however, was much smaller than that for the pyrolysis of cellulose. The fraction of phenolics decreased considerably, which was ascribed to the conversion of phenolics to aromatics on the acid sites via catalytic reforming such as decarbonylation, decarboxylation, and cracking.

When the catalyst dose was increased, the fractions of furans, mono-aromatics, and hydrocarbons, with high economic values, increased owing to enhanced cracking, dehydration, decarboxylation, decarbonylation, and aromatization occurring on acid sites. Similar to the case of cellulose, the production of furanic compounds and mono-aromatics was promoted in the presence of acid sites.

The increase in the catalyst dose led to decreased fraction of acids, indicating the conversion of acids on the acid sites. This implies that an optimal catalyst/biomass ratio would be needed to maximize the production of acids.

3.2.3. Ex situ *CP of kraft lignin*

Fig. 12 shows the results of the pyrolysis of kraft lignin. The dominant product species of the pyrolysis of lignin were phenolics because the basic structure of lignin is a network of aromatic compounds. The fraction of phenolics increased further when the pyrolysis was conducted over H-V-MCM-41 catalysts due to enhanced cracking, decarbonylation, and decarboxylation, however, bulk V_2O_5 did not affect significantly the production of phenolics. Phenolics are economically important chemicals used to produce phenolic resin. Another group of species whose fraction was increased as a result of catalytic reforming was mono-aromatics. In particular, 10 wt% H-V-MCM-41 promoted the production of mono-aromatics to the largest extent. The fraction of oxygenated aromatics, such as 1,2-dimethoxy benzene and 1-methoxy-4-methyl benzene, whose production was significant (12.2%) in the case of non-CP, was only 4.2% when the pyrolysis was conducted over 10 wt% H-V-MCM-41. This result implies the conversion of oxygenated aromatics to mono-aromatics on the acid sites of H-V-MCM-41. The conversion of phenolics to mono-aromatics on the acid sites of H-V-MCM-41 is another possibility.

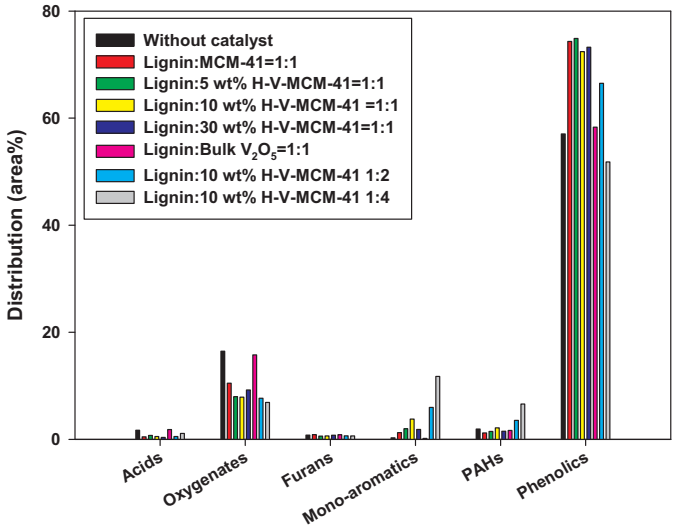

Fig. 12. Product distribution of catalytic pyrolysis of lignin over H-V-MCM-41 catalysts.

The production of alkylated phenols (including phenol), among other phenolics, was enhanced substantially due to catalytic reforming. For example, the fraction of alkyl phenol compounds increased more than four times from 3% of non-CP to 12.7% of CP over 10 wt% H-V-MCM-41. This was attributed to enhanced deoxygenation (decarbonylation and decarboxylation), cracking, and demethoxylation of primary phenolic products of thermal pyrolysis by H-V-MCM-41.

When the dose of 10 wt% H-V-MCM-41 was increased by a factor of 2 and 4, the fraction of phenolics in the product bio-oil decreased from 72.4% to 66.5% and 51.8%, respectively. Despite the reduction in total phenolic production, however, the fraction of alkylated phenols increased from 12.7% to 15.4% and 20.7%, because the functional groups of phenolic compounds (e.g. methoxy groups, carbonyl groups, etc.) were removed on the acid sites of H-V-MCM-41. For instance, the fraction of the phenolic compounds having methoxy groups (methoxy phenol, dimethoxy phenol, methoxymethyl phenol, etc.) decreased substantially from 55.1% to 48.0% and to 30.3% when the mass ratio of 10 wt% H-V-MCM-41 over lignin was increased from 1 to 2 and to 4, respectively, owing to enhanced demethoxylation and deoxygenation. The fraction of the compounds having carbonyl groups, such as hydroxy-methoxy benzaldehyde, also decreased from 8.6% for non-CP to 4.6%, 3.2%, and 0.9% for CP over 10 wt% H-V-MCM-41 with the catalyst/biomass ratio of 1, 2 and 4, respectively, due to enhanced decarbonylation (data not shown).

The increase in catalyst dose also resulted in the increases in the fractions of mono-aromatics from 3.8% to 6.0% (two-times dose) and to 11.8% (four-times dose) and polycyclic aromatic hydrocarbons (PAHs) from 2.2% to 3.6% (two-times dose) and to 6.6% (four-times dose). The fraction of oxygenated aromatics was not altered much by the change in catalyst dose, remaining at 4.2% (data not shown). Therefore, we could conclude that the increase in catalyst dose promoted the conversion of phenolics, through deoxygenation, cracking, demethoxylation, and demethylation, to mono-aromatics and PAHs as well as to alkylated phenols.

4. Conclusion

H-V-MCM-41 catalysts exhibited high catalytic activity for the reforming of pyrolysis oil from biomass components. The acid

Please cite this article in press as: B.-S. Kim, et al., *Ex situ* catalytic upgrading of lignocellulosic biomass components over vanadium contained H-MCM-41 catalysts, Catal. Today (2015), http://dx.doi.org/10.1016/j.cattod.2015.08.031

sites based on framework vanadium showed superior catalytic activity to those based on extraframework vanadium oxide. CP, compared to non-CP, led to increased production of basic chemicals needed for the petrochemical industry, e.g. furanic compounds, mono-aromatics, acetic acid, and light phenolics. In the CP of cellulose, levoglucosan, the main product of non-CP, was converted to furanic compounds, including furfural, through deoxygenation on the acid sites of catalysts. Increase in the catalyst dose and hence the increase in the quantity of acid sites led to increased production of furanic compounds, some of which were converted further to mono-aromatics. The CP of xylan, i.e. hemicellulose, over H-V-MCM-41 catalysts produced significant amount of mono-aromatics through deoxygenation, cracking, and aromatization. The production of acetic acid was also promoted by catalyst reforming through the removal of O-acetal functional groups. When kraft lignin was pyrolyzed over H-V-MCM-41 catalysts, compared to non-CP, the production of alkylated phenolics, mono-aromatics, and PAHs was promoted, which was also attributed to the effects of acid sites of the catalysts. The increase in the catalyst dose promoted the conversion reactions occurring on the acid sites, resulting in enhanced conversion of heavy phenolics having various functional groups to light alkylated phenolics and mono-aromatics. The results of this study suggest that the CP of lignocellulosic biomass over vanadium-based catalysts, such as H-V-MCM-41, can be effectively used for the production of valuable chemicals.

Acknowledgments

This work was supported by the National Research Foundation of Korea (NRF) grant funded by the Korea government (MSIP) (No. 2015R1A2A2A11001193).

References

[1] M.N.N. Shahirah, J. Gimbun, S.F. Pang, R.M. Zakria, C.K. Cheng, G.K. Chua, M.F.F. Asras, J. Ind. Eng. Chem. 23 (2015) 213.
[2] B. Klinpratoom, A. Ontanee, C. Ruangviriyachai, Korean J. Chem. Eng. 32 (2015) 413.
[3] N. Muhammad, Y.A. Elsheikh, M.I.A. Mutalib, A.A. Bazmi, R.A. Khan, H. Khan, S. Rafiq, Z. Man, I. Khan, J. Ind. Eng. Chem. 21 (2015) 1.
[4] M. Ruthiraan, N.M. Mubarak, R.K. Thines, E.C. Abdullah, J.N. Sahu, N.S. Jayakumar, P. Ganesan, Korean J. Chem. Eng. 32 (2015) 446.
[5] Q.Y. Liu, F. Yang, Z.H. Liu, G. Li, J. Ind. Eng. Chem. 26 (2015) 46.
[6] Z. Zhang, X. Feng, X.X. Yue, F.Q. An, W.X. Zhou, J.F. Gao, T.P. Hu, C.C. Wei, Korean J. Chem. Eng. 32 (2015) 1564.
[7] T.M. Abdel-Fattah, M.E. Mahmoudb, S.B. Ahmedb, N.D. Huff, J.W. Lee, S. Kumar, J. Ind. Eng. Chem. 22 (2015) 103.
[8] M. Milina, S. Mitchell, J. Pérez-Ramírez, Catal. Today 235 (2014) 176.
[9] J. Meng, A. Moore, D. Tilotta, S. Kelly, S. Park, ACS Sustain. Chem. Eng. 2 (2014) 2011.
[10] A. Heidari, R. Stahl, H. Younesi, A. Rashidi, N. Troeger, A.A. Ghoreyshi, J. Ind. Eng. Chem. 20 (2014) 2594.
[11] B. Yoosuk, J. Boonpo, P. Udomsap, S. Sukkasi, Korean J. Chem. Eng. 31 (2014) 2229.
[12] L. Zhang, R. Liu, R. Yin, Y. Mei, Renew. Sustain. Energy Rev. 24 (2013) 66.
[13] C.H. Ko, S.H. Park, J.K. Jeon, D.J. Suh, K.E. Jeong, Y.K. Park, Korean J. Chem. Eng. 29 (2012) 1657.
[14] K. Wang, P.A. Johnson, R.C. Brown, Bioresour. Technol. 173 (2014) 124.
[15] O.D. Mante, F.A. Agblevor, Green Chem. 16 (2014) 3364.
[16] X. Erdocia, R. Prado, M.Á. Corcuera, J. Labidi, J. Ind. Eng. Chem. 20 (2014) 1103.
[17] K. Wang, K.H. Kim, R.C. Brown, Green Chem. 16 (2014) 727.
[18] J.Y. Kim, H. Hwang, S. Oh, J.W. Choi, J. Ind. Eng. Chem. 30 (2015) 302.
[19] D.J. Mihalcik, C.A. Mullen, A.A. Boateng, J. Anal. Appl. Pyrolysis 92 (2011) 224.
[20] C.A. Mullen, A.A. Boateng, Fuel Process. Technol. 91 (2010) 1446.
[21] R. French, S. Czernik, Fuel Process. Technol. 91 (2010) 25.
[22] Z. Luo, S. Wang, X. Guo, J. Anal. Appl. Pyrolysis 95 (2012) 112.
[23] Z. Ma, E. Troussard, J.A. van Bokhoven, Appl. Catal. A: Gen. 423–424 (2012) 130.
[24] H. Ben, A.J. Ragauskas, ACS Sustain. Chem. Eng. 6 (2013) 316.
[25] M. Käldström, N. Kumar, D.Y. Murzin, Catal. Today 167 (2011) 91.
[26] A. Aho, M. Käldström, P. Fardim, N. Kumar, K. Eränen, T. Salmi, B. Holmbon, M. Hupa, D.Y. Murzin, Cellulose Chem. Technol. 44 (2010) 89.
[27] C. Torri, I.G. Lesci, D. Fabbri, J. Anal. Appl. Pyrolysis 85 (2009) 192.
[28] F.W. Yu, D.X. Ji, Y. Nie, Y. Luo, C.J. Huang, J.B. Ji, Appl. Biochem. Biotechnol. 168 (2012) 174.
[29] M.J. Jeon, J.K. Jeon, D.J. Suh, S.H. Park, Y.J. Sae, S.H. Joo, Y.K. Park, Catal. Today 204 (2013) 170.
[30] H.W. Lee, S.H. Park, J.K. Jeon, R. Ryoo, W. Kim, D.J. Suh, Y.K. Park, Catal. Today 232 (2014) 119.
[31] D. Fabbri, C. Torri, V. Baravelli, J. Anal. Appl. Pyrolysis 80 (2007) 24.
[32] P. Rutkowski, J. Anal. Appl. Pyrolysis 98 (2012) 86.
[33] S. Shylesh, A.P. Singh, J. Catal. 233 (2005) 359.
[34] M.R. Boccuti, K.M. Rao, A. Zecchina, G. Leofanti, G. Pentrini, Stud. Surf. Sci. Catal. 48 (1989) 133.
[35] K. Schumacher, C.D.F.V. Hohenesche, K.K. Unger, R. Ulrich, A.D. Chesne, U. Wiesner, H.W. Spiess, Adv. Mater. 11 (1999) 1194.
[36] S.B. Kim, S.J. You, Y.T. Kim, H.J. Chae, S.Y. Jeong, E.D. Park, Korean Chem. Eng. Res. 48 (2010) 684.
[37] M. Zabeti, T.S. Nguyen, L. Lefferts, H.J. Heeres, K. Seshan, Bioresour. Technol. 118 (2012) 374.
[38] T.R. Carlson, Y.T. Cheng, J. Jae, G.W. Huber, Energy Environ. Sci. 4 (2011) 145.
[39] J. Adam, M. Blazsó, E. Mészáros, M. Stöcker, M.H. Nilsen, A. Bouzga, J.E. Hustad, M. Grønli, G. Øye, Fuel 84 (2005) 1494.
[40] R. Alén, E. Kuoppala, P. Oesch, J. Anal. Appl. Pyrolysis 36 (1996) 137.

Please cite this article in press as: B.-S. Kim, et al., *Ex situ* catalytic upgrading of lignocellulosic biomass components over vanadium contained H-MCM-41 catalysts, Catal. Today (2015), http://dx.doi.org/10.1016/j.cattod.2015.08.031